THE BIOENERGETICS OF EMBRYONIC DIAPAUSE IN AN ANNUAL KILLIFISH, *AUSTROFUNDULUS LIMNAEUS*

JASON E. PODRABSKY* AND STEVEN C. HAND

Department of Environmental, Population, and Organismic Biology, University of Colorado, Boulder, CO 80309-0334, USA

*Present address: Hopkins Marine Station, Stanford University, Pacific Grove, CA 93950-3094 (e-mail: podrabsk@leland.stanford.edu)

Summary

The annual killifish *Austrofundulus limnaeus* inhabits ephemeral ponds that dry out on a seasonal basis, thereby killing the adult and juvenile forms. Populations persist because diapausing embryos become embedded in the pond sediments. The rate of oxygen consumption of diapause II embryos is depressed by up to 90 % compared with that of developing embryos, and a parallel reduction is observed in heart rate. Developmental arrest was identified by cessation of somite proliferation and blockage of the ontogenetic increase in DNA content. Surprisingly, the arrest of metabolism and development is temporally offset as embryos reach diapause II; metabolic rate begins to decline 12 days prior to arrest of development. Release of embryos from diapause II is facilitated by increasing the light phase of the photoperiod. The rate of oxygen consumption of diapause III embryos is 84 % lower than the value preceding diapause III. The total energy flow of diapause II embryos apparently includes a contribution from anaerobic processes on the basis of calorimetric/respirometric ratios that are above the oxycaloric equivalent. Accumulations of lactate and ethanol at the expense of glycogen reserves are small or undetectable and do not account for the excess heat signal. Diapause II embryos maintain high [ATP]/[ADP] ratios and adenylate energy charge during diapause, consistent with a simultaneous depression of energy use and demand. Levels of AMP increase during early development and diapause II despite the highly charged adenylate pool. High values for [AMP]/[ATP] ratios in diapause II embryos are correlated with decreased rates of oxygen consumption and heat dissipation, which suggests a role for AMP in the depression of metabolism during early development and diapause II.

Key words: calorimetry, respirometry, diapause, energetics, metabolic depression, killifish, *Austrofundulus limnaeus*.

Introduction

Annual killifish (Cyprinodontiformes, Rivulidae) occur in savanna and desert regions on the continents of Africa and South America. They inhabit ephemeral ponds in areas that experience pronounced dry and rainy seasons (Myers, 1952; Peters, 1963; Wourms, 1972a,c). *Austrofundulus limnaeus* is an annual killifish endemic to northern South America, where it is most common in the Maracaibo basin of Venezuela (Lilyestrom and Taphorn, 1982). Ponds inhabited by *A. limnaeus* dry out on a seasonal basis, killing the adult and juvenile forms (Nico and Thomerson, 1989). Populations persist in such situations as a result of the occurrence of diapause embryos embedded in the pond sediments (Myers, 1952; Wourms, 1972a,c). When the rainy season returns and the ponds again fill with water, larval fish hatch from the mud to continue the life cycle. Embryos of annual killifish may spend a considerable amount of time (the majority of their lives) in the embryonic state, enclosed in the drying mud, while they await the unpredictable return of the rainy season (Simpson, 1979). Very little is known about the physiology or biochemistry of development or diapause in annual killifish.

The goals of the present study were (1) to determine whether metabolic depression accompanies diapause in embryos of *A. limnaeus*, (2) to characterize the bioenergetic status of developing and diapausing embryos, and (3) to evaluate cues involved with the termination of diapause.

Diapause, a state of developmental arrest promoted by endogenous genetic cues, is often associated with a depression of metabolism (Levels et al., 1986; Drinkwater and Crowe, 1987; Hand, 1991; Clegg et al., 1996; Loomis et al., 1996a,b). Diapause typically precedes the onset of environmental insult and, as a result, the organism can exhibit developmental arrest and metabolic depression even under conditions considered to be optimal for development. In contrast, quiescence is a state of developmental arrest and metabolic depression induced directly by unfavorable environmental conditions. Thus, the cellular mechanisms promoting diapause *versus* quiescence are apt to be different, the former being controlled by endogenous factors (e.g. maternal effects, gene expression) and the latter by direct environmental cues (e.g. anoxia, dehydration).

Studies by Wourms (1972a–c) and Peters (1963) suggest that there is a maximum of three distinct diapause stages (diapause I, II, III) that may occur during the development of annual killifish. Diapause I occurs early in development and is associated with a unique process of annual fish development known as dispersion and reaggregation of the blastomeres (Wourms, 1972b). Diapause I is thought to be induced by unfavorable environmental conditions such as hypoxia or cold stress in *A. myersi* (Wourms, 1972c) and, consequently, may represent a form of quiescence and not true diapause. Diapause II occurs in embryos possessing 38–40 somites, a beating heart and the foundations of the central nervous system (Wourms, 1972a; J. E. Podrabsky, personal observation). Diapause III occurs just prior to hatching. The diapause III embryo is fully developed and may hatch at any time in response to the correct environmental cues. Wourms (1972a,c) reports that yolk utilization appears to stop and that heart rate is decreased drastically during diapause III. This stage has been compared with aestivation in frogs and African lungfish (Wourms, 1972c). For several biological and practical reasons, developmental arrest at diapause II was the primary focus of this study. For *A. limnaeus*, diapause II is developmentally predictable, may last for well over 100 days and is obligate; virtually no embryos can bypass this state (Wourms, 1972c). Additionally, diapause II embryos are easily identified by morphological features.

In this study, we investigate the bioenergetics of embryonic diapause in the annual killifish *A. limnaeus*. Both direct and indirect calorimetry indicate a substantial depression of metabolism in diapause II and III embryos. Calorimetric/respirometric (CR) ratios indicate a substantial contribution of anaerobic pathways to total energy flow during diapause II that cannot be accounted for by the production of lactate or ethanol at the expense of glycogen stores. Diapausing embryos maintain a highly charged adenylate pool as assessed by high [ATP]/[ADP] ratios and high values of adenylate energy charge ($[ATP]+\frac{1}{2}[ADP]/[ATP]+[ADP]+[AMP]$). [AMP]/[ATP] ratios are elevated in diapause II embryos and may play an important role in the regulation of metabolism during early development and diapause.

Materials and methods

Collection, incubation and observation of embryos

Eggs of *Austrofundulus limnaeus* were obtained through natural spawning activity of adult fish as described by Podrabsky (1999). Briefly, fish were allowed access to spawning trays containing a layer of glass beads 1–2 cm deep (500 μm diameter; Thomas Scientific, Swedesboro, USA) for 2–4 h. Trays were then transferred to a secondary container, the false bottom was removed, and the glass beads were sifted through the fiberglass screen bottom. Eggs retained on the screen were collected using a wide-mouthed plastic pipette. Each spawning event represents embryos collected from 24–26 pairs of spawning fish.

Embryos were incubated in medium formulated to mimic the ionic composition of natural ponds inhabited by *A. limnaeus* (Podrabsky et al., 1998; Podrabsky, 1999) under normoxic conditions (>70 % air saturation). Currently, little is known about the microenvironment to which embryos of *A. limnaeus* are exposed. It is likely that embryos of *A. limnaeus* will be exposed to hypoxia or anoxia at some time during their development (Podrabsky et al., 1998). Early embryos of annual killifish (prior to reaggregation of the blastomeres) are known to be tolerant of extended periods of anoxia (Peters, 1963; Wourms, 1972c). However, development through diapause II requires oxygen, and the experiments in this study were therefore all performed under normoxic conditions. The embryo medium has an osmolality of 28 mosmol kg^{-1} and is dominated by sodium chloride. Because early embryos may develop abnormally in the presence of some antibiotics (Podrabsky, 1999), these were omitted from the media for the first 2 days of development. Methylene Blue (0.0001 %) was added to the medium during this time to help reduce bacterial growth. Embryos less than 2 days old were rinsed three times with 500 ml of deionized water and then transferred to embryo medium just prior to use. At 2 days post-fertilization, embryos were treated with a 0.001 % solution of sodium hypochlorite, to help prevent fungal and bacterial infections (Podrabsky, 1999), and then transferred to embryo medium containing 10 mg l^{-1} gentamycin sulfate. Embryos were treated with 0.003 % sodium hypochlorite at least 1 h before experiments were performed.

Embryos were observed using an inverted compound microscope. A compound microscope equipped with Nomarski optics was used to obtain photographs of diapause II embryos. Synchrony of embryos within and between batches was monitored between 12 and 26 days post-fertilization by determining the mean number of somites present per embryo. Heart rate was estimated from observations over 2 min intervals. During observations, temperature was held constant at 25 °C using a water-jacketed slide. A blue-filtered tungsten light source of low intensity was used for illumination to avoid radiant heating of the embryos.

Alterations in the photoperiod experienced by embryos were evaluated as a mechanism for synchronizing termination of diapause II. The light:dark cycle was manipulated while holding the temperature constant at 25 °C. Fluorescent light provided illumination. Embryos were examined every 3 days to determine the percentage of embryos that had broken diapause. Diapause II was considered to be broken when circulation of red blood cell precursors was observed.

Metabolic profiles

Each batch of embryos was divided into two groups for concurrent measurements of rates of oxygen consumption and heat dissipation. Oxygen consumption was determined using polarographic oxygen electrodes (model 1302; Strathkelvin Instruments, Glasgow, Scotland) in a water-jacketed respirometry chamber (model 350; Strathkelvin Instruments). Data were collected using DataCan V data acquisition software (Sable Systems, Las Vegas, USA). Samples of 30–70 embryos

were assayed in 1.5 ml of air-saturated embryo medium containing 10 mg l⁻¹ gentamycin sulfate. Each group of embryos was assayed twice, and the values were averaged to provide one *N* value (*N*=independent spawning event). Oxygen consumption was recorded for 10–70 min depending on the developmental stage. Oxygen tension in the chamber was maintained at greater than 80 % air saturation. Measurements were made under ambient light conditions at 25 °C. No differences were observed between rates of oxygen consumption of embryos in the dark or light (data not shown). Oxygen consumption data were analyzed using DatGraf software (Cyclobios, Innsbruck, Austria) as described by Kwast et al. (1995) to correct for oxygen consumption by the electrodes, back diffusion into the system and the time constants for the electrodes.

Heat dissipation was measured by direct calorimetry in a closed 5 ml ampoule using a thermal activity monitor (model 2277; LKB, Bromma, Sweden). Depending on the developmental stage, groups of 5–130 embryos were used for each estimation of heat dissipation. All determinations were made at 25 °C. Embryos were immersed in 4 ml of embryo medium containing 10 mg l⁻¹ gentamycin sulfate that had been equilibrated to a gas mixture of 40 % oxygen and 60 % nitrogen. The elevated level of oxygen prevented embryos from becoming hypoxic in the absence of stirring. After allowing the instrument to stabilize following the introduction of the ampoule (25 min), time-corrected data were collected at 1 min intervals using a QuickBasic program. Heat dissipation was averaged over a 0.5–1 h collection period. Calorimetric/respirometric (CR) ratios (kJ mol O_2^{-1}) were calculated from oxygen consumption and heat dissipation data collected independently, but from the same batch of embryos. Theoretical oxycaloric equivalents were taken from Gnaiger (1983) and Widdows (1987).

Metabolite extraction

At selected time points during development, 50 embryos from each of four independent spawning events were flash-frozen in liquid nitrogen, pulverized and extracted in 750 µl of ice-cold 1 mol l⁻¹ perchloric acid containing 5 mmol l⁻¹ EDTA (Lowry and Passonneau, 1972). The homogenate was divided into two subsamples and centrifuged at 10 000 *g* for 10 min at 4 °C. The supernatants were combined and neutralized with 5 mol l⁻¹ K_2CO_3. The neutralized supernatant was centrifuged at 10 000 *g* for 10 min at 4 °C to remove perchlorate salts. A sample of the resulting supernatant was removed and combined with two volumes of 95 % ethanol (−20 °C) and stored at −20 °C for 15–20 h to precipitate glycogen. The remaining supernatant was frozen in liquid nitrogen and stored at −80 °C. The acid-insoluble pellet from one subsample was resuspended in 0.5 mol l⁻¹ NaOH for determination of total protein. The second acid-insoluble pellet was resuspended in 0.5 mol l⁻¹ perchloric acid for determination of total DNA. All samples were stored at −80 °C until analyses were performed.

Biochemical analyses

ATP, ADP and AMP concentrations were determined by reverse-phase high-performance liquid chromatography (HPLC; Milton Roy CM4000 series) as described by Rees and Hand (1991) with the modifications outlined by Kwast and Hand (1996). Separations were achieved using an amino-propyl silica column (Sphereclone, 250 mm×4.6 mm, 5 µm particle size, Phenomenex, Torrance, USA). The mobile phase consisted of 65 mmol l⁻¹ potassium phosphate (pH 6.5) and acetonitrile (1:2.15, v/v). Samples were filtered (0.45 µm) prior to injection and eluted isocratically at a flow rate of 1.75 ml min⁻¹. Absorbance was measured at 254 nm. Peaks corresponding to adenylates were verified by co-elution with known standards and quantified by integration of peak area. IMP was not resolvable using this system because of interference from a large unknown peak.

Glycogen content was determined using a modified anthrone assay (Jermyn, 1975) as described by Carpenter and Hand (1986). The ethanol-fractionated samples were thawed on ice and centrifuged at 12 000 *g* for 20 min at 4 °C. The pellets were washed once in 95 % ethanol, dried for 5 min at medium heat in a DNA speed vacuum (Savant Instruments, Farmingdale, USA) and redissolved by heating at 70 °C in deionized water. Glycogen content was expressed in glucosyl units. Lactate concentration was determined enzymatically using the lactate dehydrogenase reaction. The reaction was monitored by following the appearance of NADH at 340 nm (Bergmeyer, 1974). Final concentrations of reagents in the 1 ml assay mixture were: 0.6 mol l⁻¹ glycine, 0.5 mol l⁻¹ hydrazine, 2.7 mmol l⁻¹ NAD⁺ and 14 units of lactate dehydrogenase (pH 9.2). Ethanol was measured spectrophotometrically using the alcohol dehydrogenase reaction as described by Bergmeyer (1974).

Total protein content was measured in acid-insoluble pellets (resuspended in 0.5 mol l⁻¹ NaOH) using a modified Lowry protein assay (Peterson, 1977). Bovine serum albumin served as the standard. A diphenylamine assay (Burton, 1956), as modified by Giles and Myers (1965), was used to quantify total DNA. Perchloric-acid-insoluble pellets were brought to a final concentration of 1.5 mol l⁻¹ perchloric acid, and the suspension was heated at 75 °C for 30 min to digest the DNA. The samples were centrifuged at 10 000 *g* for 10 min at 4 °C. A 1 ml sample of the supernatant was combined with 1 ml of 4 % diphenylamine prepared in glacial acetic acid. Finally, 0.05 ml of 1.6 mg ml⁻¹ aqueous acetaldehyde was added, and the samples were incubated at 30 °C for 20 h. Color development was measured at 595 nm. To correct for non-specific color development and turbidity, the absorbance at 700 nm was subtracted from the absorbance at 595 nm for each sample or standard (Giles and Myers, 1965). Highly polymerized DNA (bovine calf thymus) dissolved in 5 mmol l⁻¹ NaOH served as a standard.

Expression of biochemical data

Normalization of biochemical data is difficult in embryonic systems because of the continual increase in cellular mass at the expense of yolk stores. Biochemical constituents that are distributed primarily in the embryonic cells (e.g. adenylates, see Results and Discussion) may be best expressed per

microgram of DNA. Expressing the adenylate data per unit of DNA probably provides a more biologically meaningful pattern because it reflects the cellular proliferation of metabolically active tissue. Normalization to DNA content does not account for changes in cell volume, but cell volume does not appear to change substantially after late reaggregation in embryos of *A. myersi* (compare Figs 10 and 11 in Wourms, 1972b). It may be reasonable to assume a similar situation for embryos of *A. limnaeus* after 8 days post-fertilization. Biochemical constituents that are known to be distributed in both the yolk and the embryo are more appropriately expressed per gram wet mass. Data expressed per gram wet mass and per embryo yield similar patterns in early embryos of *A. limnaeus* as a result of the very slight change in the wet mass of embryos between 0 and 70 days post-fertilization (data not shown). Expressing data per milligram protein for early embryos of *A. limnaeus* may be misleading because of a 22 % decrease in total protein during development (see Results). Additionally, there is an overall small mass of embryonic cells compared with a large mass of proteinaceous yolk in diapause II embryos (see Results).

Statistical analyses

All statistical calculations were performed using SAS software (SAS Institute, Cary, USA). CR ratios were compared with the theoretical oxycaloric equivalent for a mixed metabolism ($-450\,\mathrm{kJ\,mol^{-1}\,O_2}$) with a one-sample *t*-test using the oxycaloric equivalent as the parametric value. Analysis of covariance (ANCOVA) was used to evaluate the effect of different photoperiod regimes on the termination of diapause II. Correlation analysis was selected to evaluate the relationship between [AMP]/[ATP] ratios and both indices of metabolic rate. Analysis of variance (ANOVA) was used to compare all other data sets. Tukey's HSD test was adopted for comparisons among specific means within a data set. Means were considered statistically different at $P<0.05$.

Results

Developmental pattern and diapause states

Embryos of *A. limnaeus* undergo substantial changes in cell number, complexity and mass of metabolically active tissue during development. The embryonic axis first forms at approximately 10 days post-fertilization. After 12 days post-fertilization, pairs of somites are added at a regular rate of approximately $3\,\mathrm{day^{-1}}$ until entry into diapause II (Fig. 1). Another useful indicator of developmental progress is the formation of a functional heart, which occurs at approximately 14 days post-fertilization. Heart rate increases rapidly and reaches a maximum value of $27.9\pm1.8\,\mathrm{beats\,min^{-1}}$ (mean ± S.E.M., $N=7$) at 18 days post-fertilization (Fig. 1). Total DNA content was measured to provide an index proportional to cell number (Fig. 2A). Day zero embryos (2–4 cell stage) contain $44.1\pm3.0\,\mathrm{\mu g\,DNA\,g^{-1}}$ wet mass (mean ± S.E.M., $N=4$). This value increases steadily through early development and reaches a maximum of $168.5\pm4.2\,\mathrm{\mu g\,DNA\,g^{-1}}$ wet mass at 20 days post-fertilization. There is a statistically significant drop in protein content from $94.5\pm1.5\,\mathrm{mg\,g^{-1}}$ wet mass (mean ± S.E.M., $N=4$) at zero days post-fertilization to $73.9\pm3.1\,\mathrm{mg\,g^{-1}}$ wet mass at 70 days post-fertilization (Fig. 2B).

A. limnaeus embryos reared in our laboratory do not arrest at diapause I (dispersed cell stage, approximately 4 days post-fertilization) under aerobic conditions (J. E. Podrabsky personal observation). Rather, only two distinct diapause stages occur under aerobic conditions, diapause II and III (Fig. 3; Podrabsky, 1999). At the onset of diapause II (24–26 days post-fertilization), the developmental proliferation of somites is arrested at 38 pairs (Fig. 1). Heart rate declines from
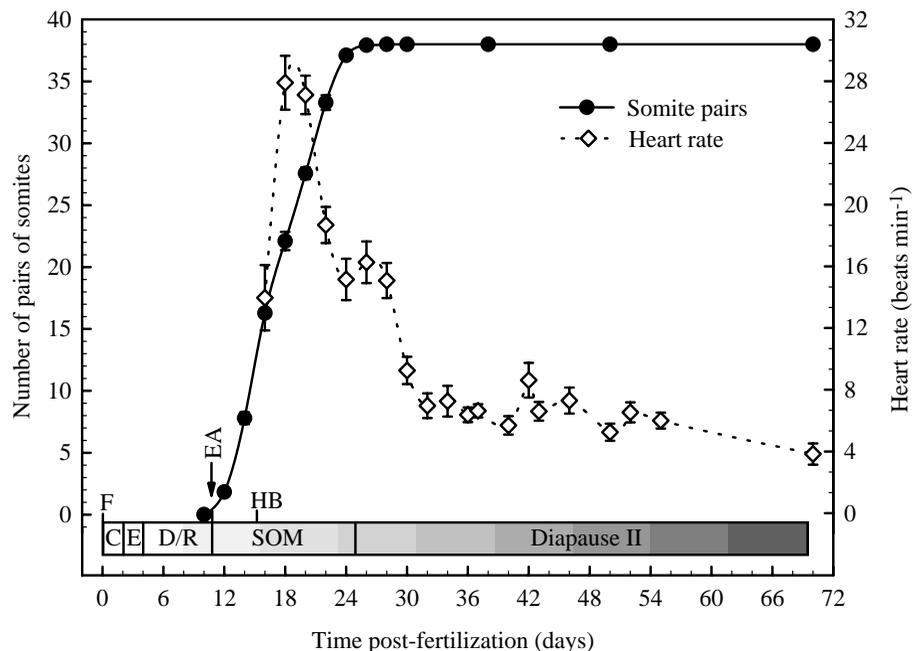

Fig. 1. Number of somite pairs (mean ± S.E.M., $N=3–7$) and heart rate (mean ± S.E.M., $N=30$) as a function of development through diapause II in embryos of *Austrofundulus limnaeus*. The gray scale bar indicates the timing of major developmental events. F, fertilization; C, cleavage; E, epiboly; D/R, dispersion and reaggregation of the blastomeres; EA, formation of the embryonic axis; SOM, somitogenesis; HB, first indication of a heart beat.
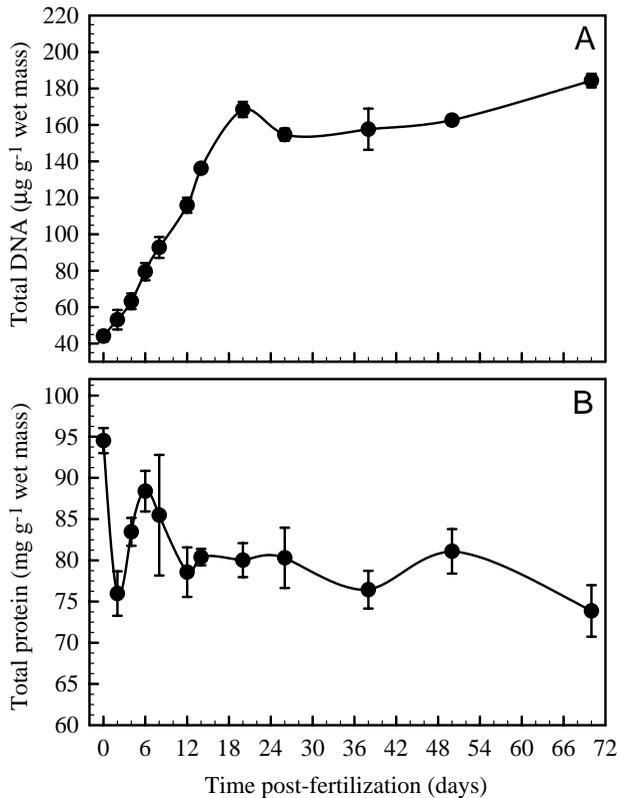
observation period. Several of these embryos were observed for up to 10 min, but heart function was still not evident. The ontogenetic increase in DNA content is also blocked during diapause II (Fig. 2A).

The morphology of diapause II and III embryos is illustrated in Fig. 3. Diapause II embryos are dominated by the presence of yolk material (Fig. 3A), which represents approximately 90 % of the total embryo mass. While the foundations of the central nervous system, sensory systems, circulatory system and precursors for muscle and bone (somites) have all formed (Fig. 3C), the major periods of organogenesis have not yet occurred in diapause II embryos. In contrast, diapause III embryos (Fig. 3B) have completed embryonic development and depleted nearly all the yolk stores. *A. limnaeus* embryos hatch into precocial larvae that immediately begin feeding.

Environmental cues that promote the release of embryos from diapause are probably multifaceted. However, we show here that alterations in photoperiod can facilitate the breakage of diapause. Specifically, lengthening the light phase promotes a significantly more rapid termination of diapause II (ANCOVA, P=0.0001; Fig. 4). A long-day photoperiod (14 h:10 h L:D) has the greatest effect on breakage of diapause, while the 10 h:14 h L:D (short-day) photoperiod elicits an

its maximum of 28 beats min^{-1} to mean values as low as 3.8±0.7 beats min^{-1} (mean ± S.E.M., N=30 embryos) during diapause. It is worth noting that 23 % of the embryos at 70 days post-fertilization exhibited no heart function during the 2 min
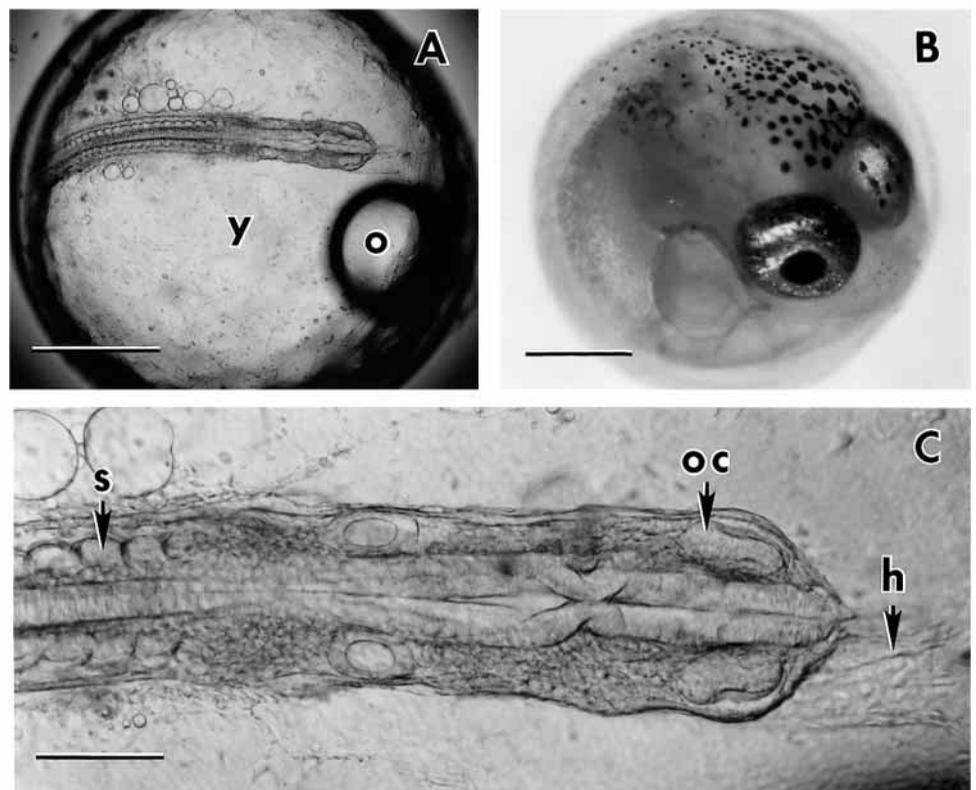

Fig. 3. Photomicrographs (Nomarski optics) of a diapause II embryo (A,C) and a diapause III embryo (B) of *Austrofundulus limnaeus*. In A, y marks the large yolk mass, while o marks the oil droplet. In C, h points to the heart, oc to an optic cup and s to a somite. Scale bars, 500 µm in A and B, and 115 µm in C.
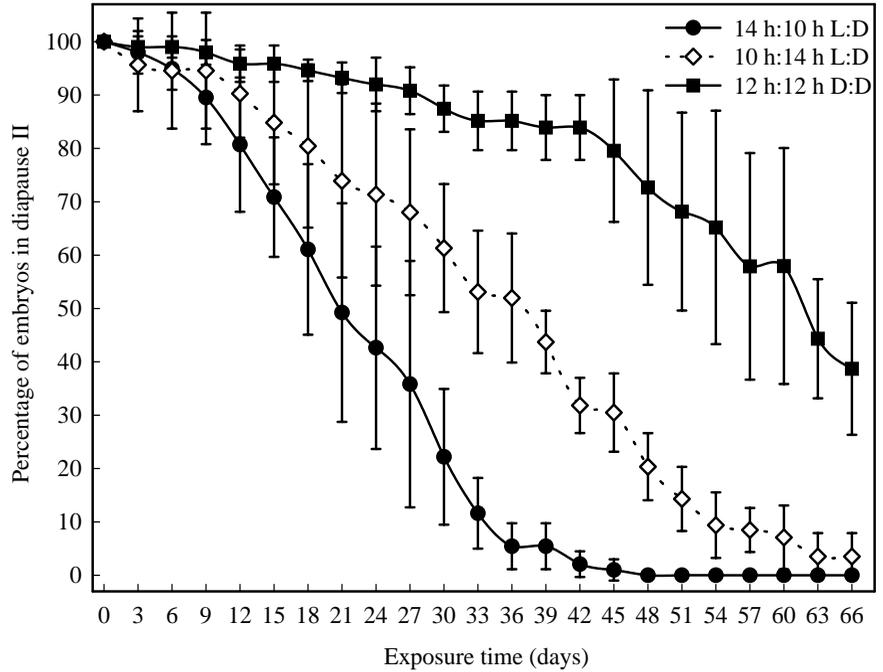
Fig. 4. Influence of photoperiod on diapause II breakage in embryos of *Austrofundulus limnaeus*. Increased duration of the photophase causes an acceleration of diapause II breakage. Values are means ± S.E.M. (*N*=3).

intermediate effect compared with controls kept in complete darkness.

Metabolism during development and diapause

The rate of oxygen consumption and heat dissipation in early embryos of *A. limnaeus* peak at 8 days post-fertilization (Fig. 5). Developmentally, this age corresponds to the reaggregation of the blastomeres, but with no formation of an embryonic axis (see Fig. 1). The rate of oxygen consumption and heat dissipation then decline more or less continuously as the embryos continue to develop and then enter diapause II

(24 days post-fertilization). At this stage, embryonic oxygen consumption is already depressed by almost 70 % compared with rates at 8 days post-fertilization. The rate of heat dissipation at 24 days post-fertilization is depressed by 67 % compared with rates at 8 days post-fertilization. Thus, both indicators of metabolic rate show a major depression of energy flow prior to entry into diapause II as defined by the onset of developmental arrest. An additional decline in the rate of oxygen consumption is observed during diapause II (Tukey's HSD, comparing values at 24 days post-fertilization with values at 50 days post-fertilization). The rate of oxygen
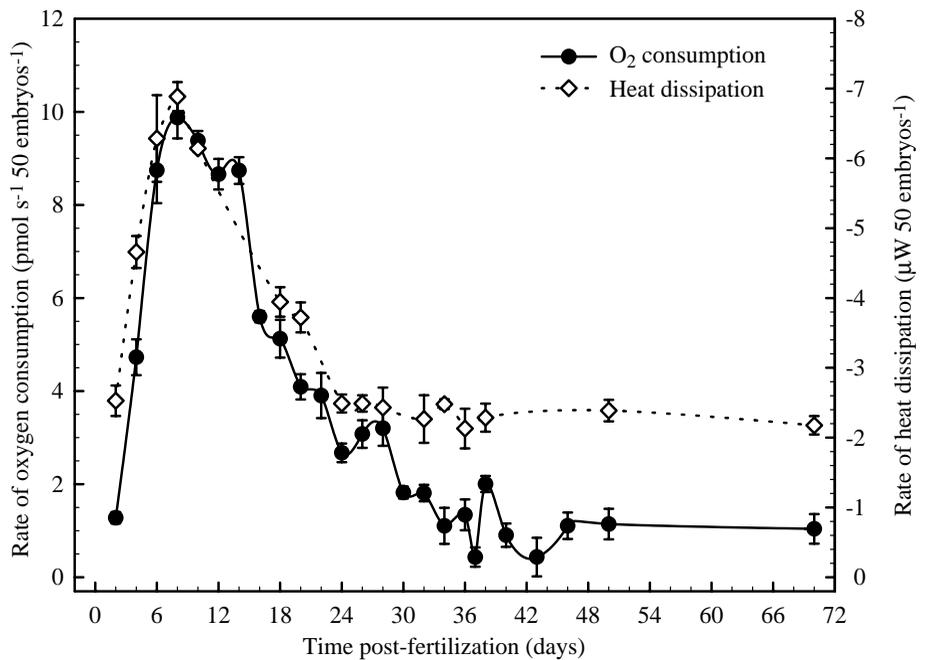

Fig. 5. Rates of oxygen consumption and heat dissipation as a function of development through diapause II in embryos of *Austrofundulus limnaeus*. Embryos enter diapause II at 24–26 days post-fertilization. Symbols represent the mean ± S.E.M. (*N*=4–10 independent spawning events for oxygen consumption and *N*=4 for heat dissipation).

Fig. 6. Calorimetric/respirometric (CR) ratios for embryos of *Austrofundulus limnaeus* as a function of development through diapause II compared with the theoretical oxycaloric equivalent for a mixed-substrate metabolism (dashed line). Columns represent the mean + S.E.M. ($N=4$ independent spawning events). Columns marked with an asterisk are significantly different from the theoretical oxycaloric equivalent ($-450\,\mathrm{kJ\,mol^{-1}}\,O_2$; *t*-test, $P<0.05$).
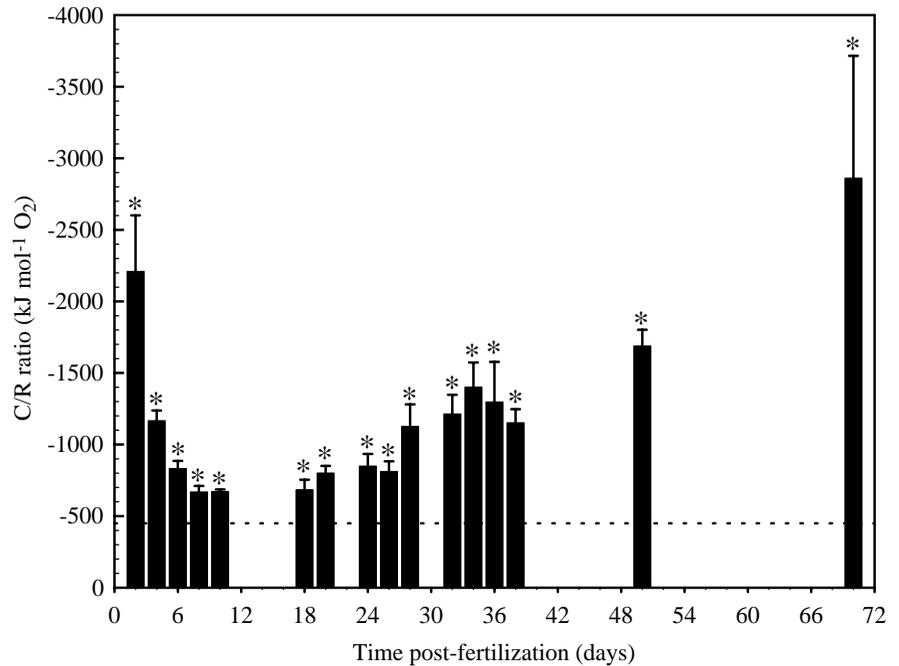
consumption in 70 days post-fertilization embryos is depressed by 90 % compared with embryos at 8 days post-fertilization and by 67 % compared with embryos at 24 days post-fertilization. This additional decline in the rate of oxygen consumption is not accompanied by a concomitant decrease in the rate of heat dissipation. This pattern is reflected by the elevated CR ratios observed in diapause II, where a maximum value of $-2860\pm855\,\mathrm{kJ\,mol^{-1}}\,O_2$ (mean $\pm$ S.E.M., $N=4$) is reached at 70 days post-fertilization (Fig. 6).

Upon release from diapause II and resumption of development, energy flow increases steeply over the next 15–20 days (Fig. 7). The rate of oxygen consumption is almost 10-fold higher after 3 days of post-diapause II development, and 64-fold higher after 9 days. The maximum rate of oxygen consumption is reached after 21 days of post-diapause II development (the late, pre-hatching embryo) and is over 200-fold greater than rates observed during diapause II. Embryos that fail to hatch by 21 days post-diapause II, enter diapause III. Rates of oxygen consumption and heat dissipation slowly decline during diapause III. When the experiment was terminated at 75 days post-diapause II, values for oxygen consumption and heat dissipation were
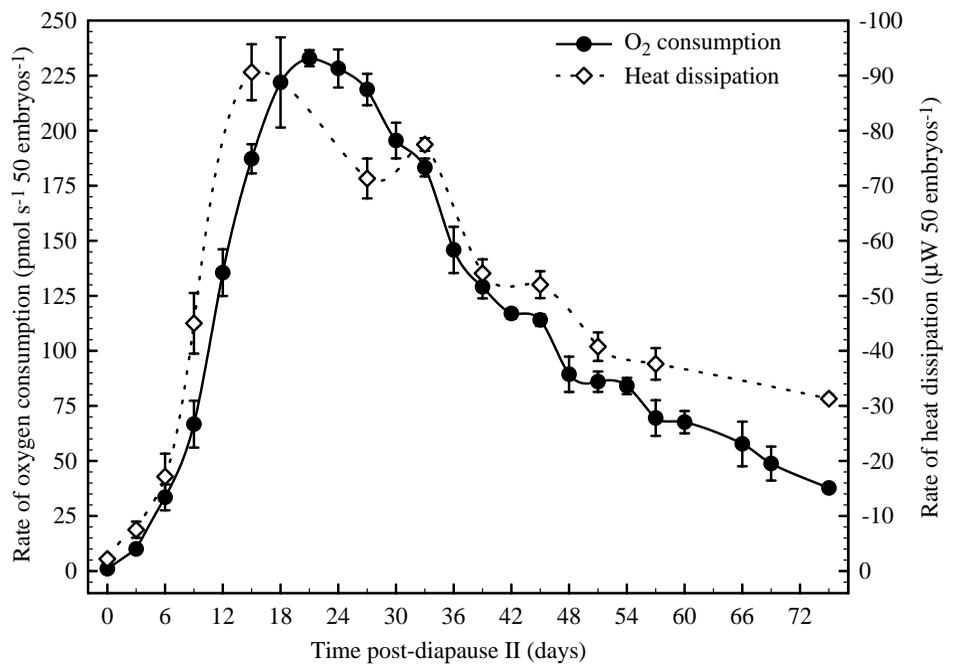

Fig. 7. Rates of oxygen consumption and heat dissipation increase after breakage of diapause II in embryos of *Austrofundulus limnaeus*. Zero days post-diapause II corresponds to 70 days post-fertilization. Embryos enter diapause III at 21–24 days post-diapause II. Symbols represent means $\pm$ S.E.M. ($N=4$ independent spawning events).
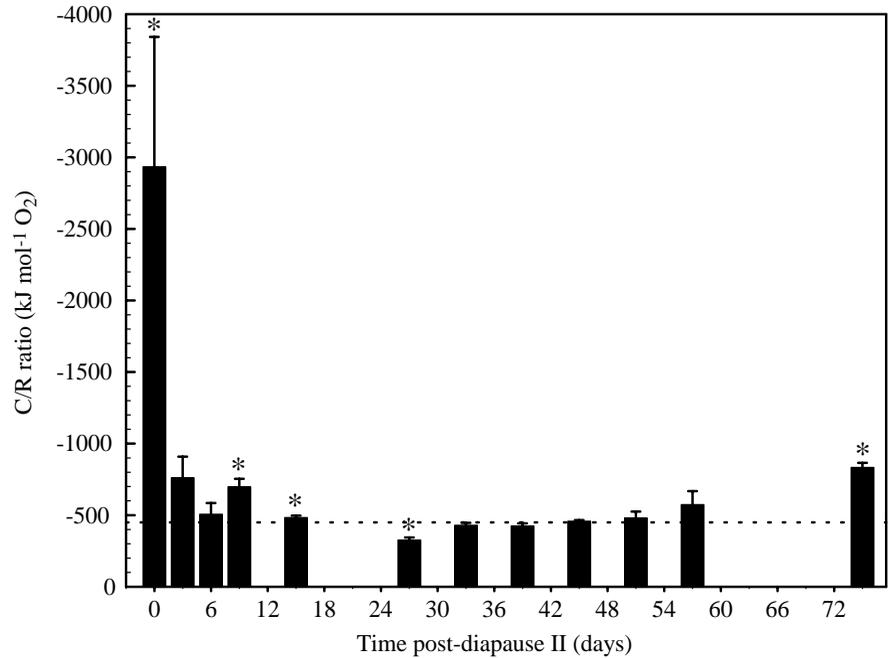
Fig. 8. Calorimetric/respirometric (CR) ratios for post-diapause II metabolism of *Austrofundulus limnaeus* embryos. Columns represent means + S.E.M. (*N*=4). Columns marked with an asterisk are significantly different (*t*-test, *P*<0.05) from the oxycaloric equivalent for mixed-substrate metabolism (dashed line; −450 kJ mol^{-1} O$_2$).

37.7 ± 1.4 pmol O$_2$ s^{-1} 50 embryos^{-1} (mean ± S.E.M., *N*=4) and -31.3 ± 0.7 μW 50 embryos^{-1}, respectively. This rate of oxygen consumption is depressed by 84 % compared with peak rates of oxygen consumption in embryos at 21 days post-diapause II. Profiles of heat dissipation are similar to those for respiratory metabolism during post-diapause II development and diapause III. Post-diapause II metabolism is largely aerobic, as indicated by CR ratios that are mostly indistinguishable from the theoretical oxycaloric equivalent for aerobic metabolism of mixed substrates (Fig. 8). CR ratios increase slightly during late diapause III, which suggests a small contribution of anaerobic pathways to total energy flow in late diapause III embryos.

Adenylates, glycogen and end products

Levels of total adenine nucleotides (ATP, ADP, AMP), expressed in nmol g^{-1} wet mass, increase significantly (ANOVA, *P*=0.0001) during early development and remain stable and high during diapause II (Fig. 9A). However, when expressed as a function of total DNA content, total adenylates decrease significantly (ANOVA, *P*=0.0001) during this same period (Fig. 9B). Two distinct phases can be distinguished with respect to the content of total adenylates when expressed per unit of DNA. During the first 6 days of development (the period of rapid cell division and major cell movements), total adenylates decrease per unit DNA. After this point, total adenylates per unit DNA (per cell) remain constant despite an increase in total DNA content (cell number) through entry into diapause II.

Fig. 9. (A) Levels of total adenine nucleotides (ATP, ADP, AMP) expressed per gram wet mass during development through diapause II for embryos of *Austrofundulus limnaeus*. (B) Total adenylate levels expressed per microgram DNA. Values are means ± S.E.M. (*N*=4 independent spawning events).

ATP content per microgram DNA decreases significantly during the first 8 days of development and then decreases more slowly for the duration of development and diapause II (Fig. 10A). Levels of ADP follow a similar trend to those for ATP, but reach stable values at 2 days post-fertilization (Fig. 10B). AMP levels rise initially, fall to extremely low values at 8 days post-fertilization, and then rise significantly as
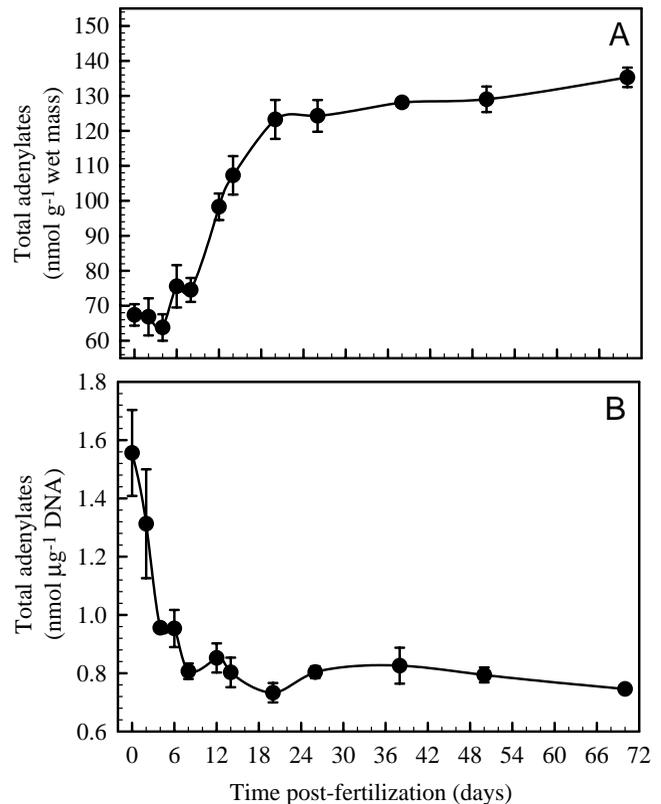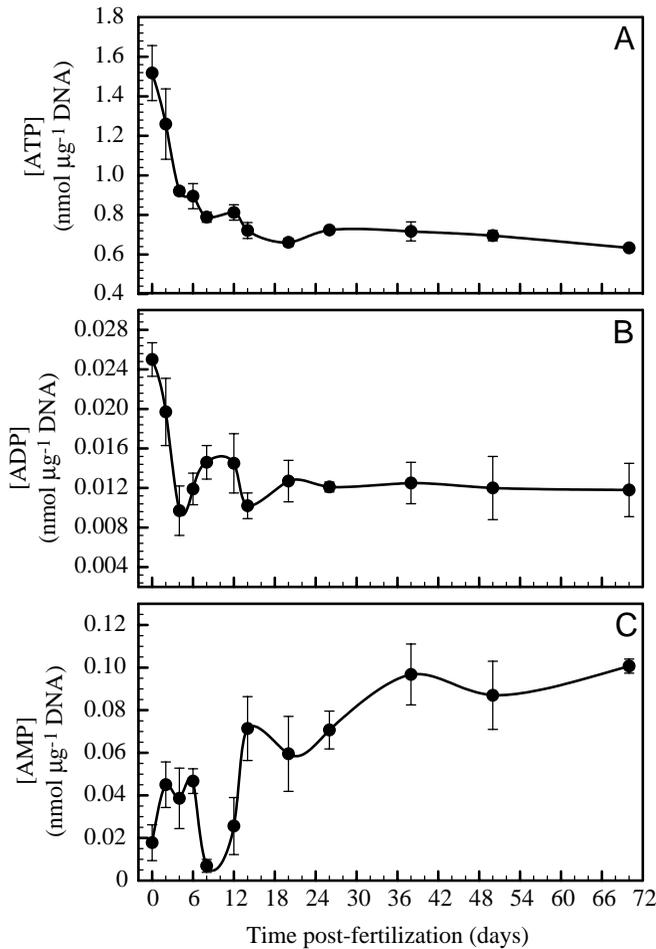
Fig. 10. Levels of ATP (A), ADP (B) and AMP (C) in embryos of *Austrofundulus limnaeus* during development through diapause II. Values are means ± s.e.m. (*N*=4 independent spawning events).
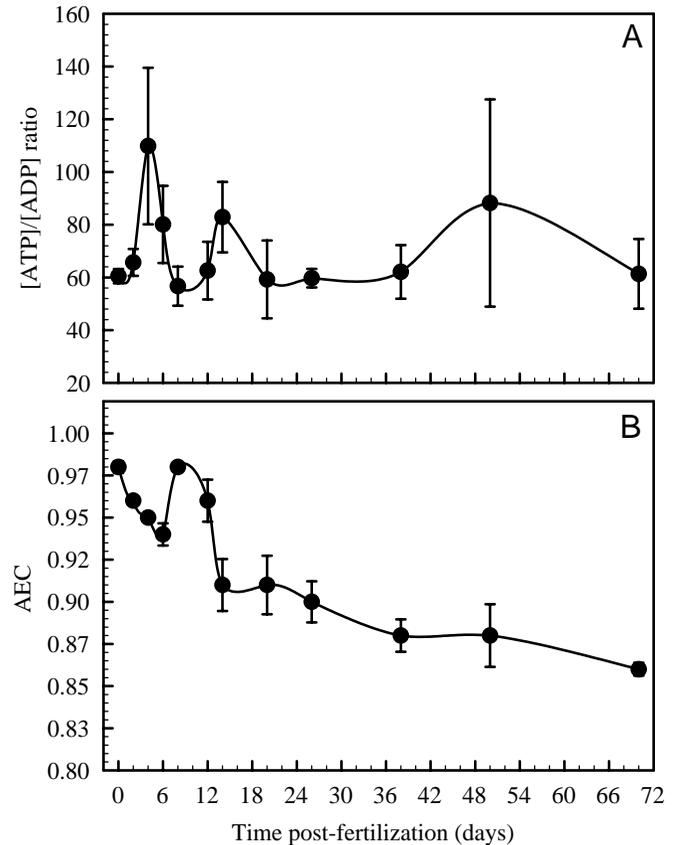

Fig. 11. (A) [ATP]/[ADP] ratios and (B) adenylate energy charge (AEC) for embryos of *Austrofundulus limnaeus* during development through diapause II. Symbols represent means ± s.e.m. (*N*=4 independent spawning events).

the embryos progress towards diapause II (Fig. 10C). At 70 days post-fertilization, levels of AMP reach a maximum of 0.10±0.003 nmol µg^{-1} DNA (mean ± s.e.m., *N*=4). [ATP]/[ADP] ratios are high (≥50) during early development and diapause II (Fig. 11A). No significant relationship was found between [ATP]/[ADP] ratios as a function of development. Values for adenylate energy charge also remain high during diapause, although a statistically significant decrease from 0.99 to 0.88 is observed between 8 and 38 days post-fertilization (Fig. 11B). This decrease in adenylate energy charge is explained by the increase in [AMP] during this period. Because of the potential importance of [AMP]/[ATP] ratio in the regulation of biosynthetic activity (see Discussion), we also evaluated these data using this metric. [AMP]/[ATP] ratios increase significantly from 8 days post-fertilization through diapause II (Fig. 12A). There is a strong negative correlation between the [AMP]/[ATP] ratio and both the rate of oxygen consumption (*r*=−0.852, *P*=0.0035) and the rate of heat dissipation (*r*=−0.934, *P*=0.0021; Fig. 12B).

Finally, glycogen content does not change significantly as a function of development (Fig. 13A). Lactate level is initially low in two- to four-cell stage embryos and increases significantly to a maximum of approximately 5 µmol g^{-1} wet mass at 4 days post-fertilization (Fig. 13B). Levels of lactate then decline as development proceeds through diapause II. However, after 20 days post-fertilization, there is no significant change is levels of lactate. Ethanol was not detected in perchloric acid extracts of developing or diapause II embryos or in the media in which these embryos were bathed (data not shown).

Discussion

In the present study, we evaluate the bioenergetics of embryonic diapause in an annual killifish. The metabolism of diapause II and III embryos is substantially depressed compared with that of developing embryos. Arrest of metabolic rate and developmental progression are temporally offset during pre-diapause II development; metabolic rate begins to decline 12 days prior to developmental arrest at diapause II, despite significant increases in total DNA content and embryonic complexity. The total energy flow of diapause II embryos appears to include a contribution from anaerobic processes, even though the embryos are incubated under
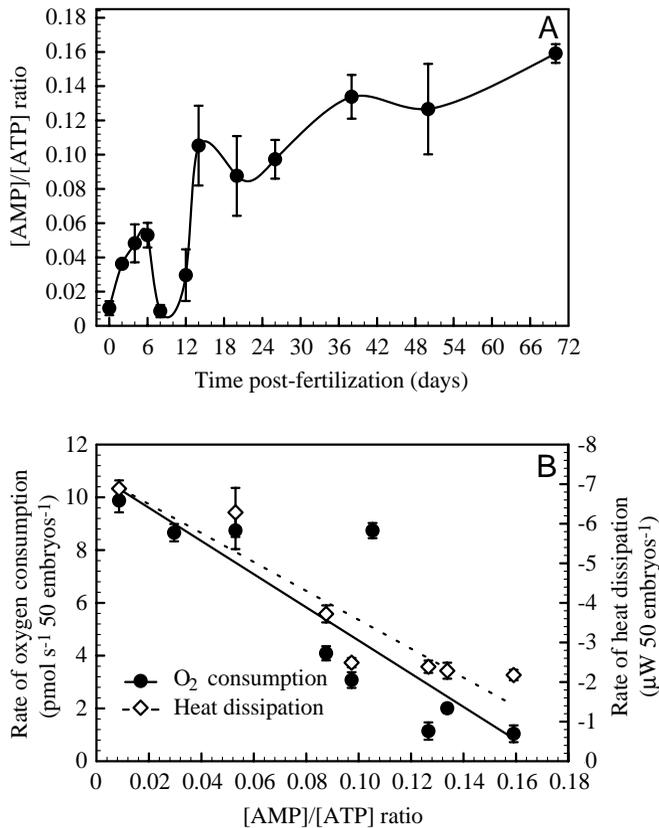
Fig. 12. (A) [AMP]/[ATP] ratios for embryos of *Austrofundulus limnaeus* as a function of development through diapause II. (B) Correlation between [AMP]/[ATP] ratios and rates of oxygen consumption and heat dissipation. Values are means ± S.E.M. (*N*=4 independent spawning events).
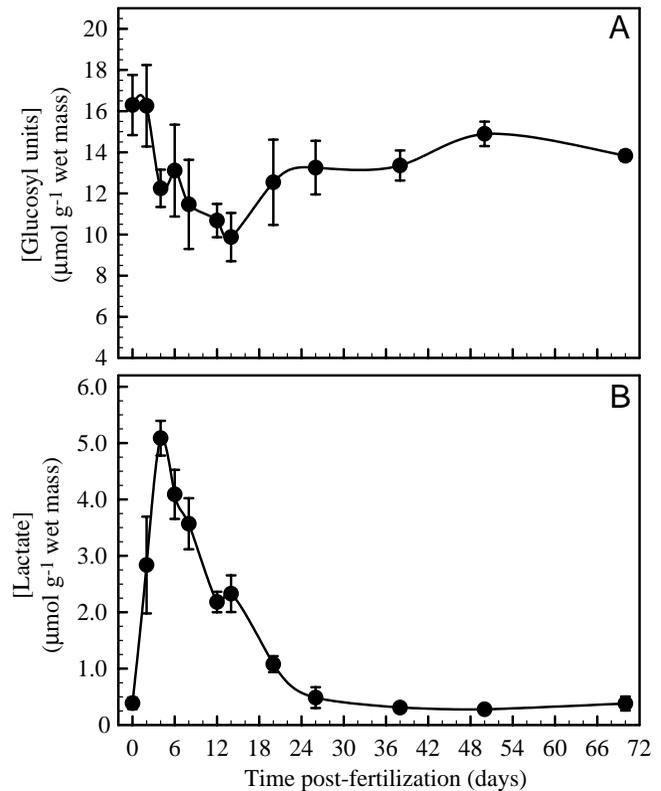

Fig. 13. (A) Glycogen content (expressed as glucosyl units) during development through diapause II in *Austrofundulus limnaeus* embryos. (B) Lactate levels as a function of development over the same time period. Values are means ± S.E.M. (*N*=4 independent spawning events).

normoxic conditions. Accumulation of typical anaerobic end products, such as lactate and ethanol, at the expense of glycogen reserves cannot account for the unexplained heat signal. Diapause II embryos maintain a highly charged adenylate pool, which suggests that catabolic and anabolic processes are down-regulated in a coordinated fashion during this transition. High [AMP]/[ATP] ratios are correlated with the decreased rates of energy flow observed in diapause II embryos, suggesting that elevated levels of AMP may contribute to the depression of metabolism during early development and diapause in *A. limnaeus*.

Metabolic profiles
Early development and diapause II

The decline in rates of oxygen consumption and heat dissipation beginning at 8 days post-fertilization (12 days prior to the onset of diapause II) was an unexpected result (Fig. 5). In general, rates of respiration and heat dissipation tend to increase continually during early development in fish (Hishida and Nakano, 1954; Milman and Yurowitzky, 1973; Boulekbache, 1981; Walsh et al., 1989; Paynter et al., 1991; Finn et al., 1995). Walsh et al. (1989) report a slight decrease in the rate of oxygen consumption between early epiboly and

the formation of the embryonic axis in the striped mullet *Mugil cephalus*. However, after the formation of the embryonic axis, the rate of oxygen consumption increases continually for the duration of early development (Walsh et al., 1989). While the basis for the decline in the rate of energy flow starting at 8 days post-fertilization is unclear, we propose two hypotheses that may explain this pattern. First, the decline may not be associated with entry into diapause but, rather, may be due to the unique developmental pattern of annual killifish. In *A. limnaeus* and other annual killifish, the cell movements associated with epiboly (cell migration of the blastoderm around the yolk) are separated from the formation of an embryonic axis (Wourms, 1972a,b), and perhaps the separation of these two processes can explain the decline in metabolic rate that occurs shortly after the major cell migrations have occurred and the embryonic axis forms. In most teleosts, epiboly and embryonic axis formation occur simultaneously. Thus, separating the contribution of each process to the total metabolism of the embryo is difficult, if not impossible. The cell movements during epiboly may account for a large proportion of the metabolic rate associated with epiboly, while the formation of the embryonic axis may require considerably less energy. An alternative hypothesis is that the metabolic decline is strictly associated with diapause and may be

explained by a sequential exit of dividing cells from the cell cycle in an anterior-to-posterior fashion. This hypothesis is based on the observation that the development of fish (and most vertebrates) occurs in an anterior-to-posterior direction. Thus, while major developmental processes may be complete in the anterior region, the posterior region may still be developing. Such a pattern could explain how somites are still being added in the posterior region until 24 days post-fertilization, yet metabolic rate is already declining after 8 days post-fertilization (as a result of cell cycle arrest in the more anterior regions). Information on the energy metabolism and developmental patterns of annual killifish species that do not enter diapause II may help to clarify this point.

After embryos of *A limnaeus* reach diapause II, rates of oxygen consumption continue to decline for an additional 8–10 days (Fig. 5). A slow decline in metabolic rate appears to be a common trait of diapause embryos. Levels et al. (1986) report that embryos of the African annual killifish *Nothobranchius korthausae* reach a minimum rate of oxygen consumption only after 3 weeks of diapause II. Clegg et al. (1996) have shown in the brine shrimp *Artemia franciscana* that metabolic rate slowly declines upon entry into diapause over a period of 5 days. Loomis et al. (1996a,b) have found a depression of metabolic rate in diapause sponge gemmules, but no time course data are reported.

Light-induced termination of diapause II

The ecological significance of light-induced termination of diapause II (Fig. 4) is not fully clear, but there are a number of reasons to believe that this response may be ecologically relevant. Other investigators have found that photoperiod can affect the occurrence of diapause in embryos of African annual killifish (Markofsky and Matias, 1977; Markofsky et al., 1979; Levels and Denucé, 1988). Exposure to light may occur in two situations. First, the embryos may receive light cues while encased in dry mud, which could serve to activate the embryos prior to the return of the rainy season. Light has been shown to penetrate up to 20 mm through sandy soils and up to 2 mm in silt- and clay-dominated soils (for a review, see Tester and Morris, 1987). Although less than 1 % of the incident light is likely to pass farther than a few millimeters into the soil, this small amount of light is known to be important in light-stimulated seed germination and root geotropism (Tester and Morris, 1987). In addition, embryos of *A. limnaeus* are found in soils that crack substantially during the dry season, increasing the chance of light penetration (Leslie, 1965, as cited by Mandoli et al., 1990). Second, during heavy rains, embryos may be mixed into the water column. Exposure to light in this situation could serve to synchronize the resumption of development with water availability.

Late development and diapause III

The metabolic rate of post-diapause II embryos increases rapidly and peaks at approximately 21 days post-diapause II (Fig. 7). At this time, embryos can hatch spontaneously or can be induced to hatch by slight manipulations in light level,

temperature or oxygen concentration. Embryos that fail to hatch during this time enter diapause III. Diapause III embryos exhibit a slow decline in metabolic rate over time. Although the experiment was terminated at 75 days post-diapause II, it appears that further declines in rates of oxidative metabolism are probable with increasing time spent in diapause III. Levels et al. (1986) report similar rates of oxygen consumption for diapause III embryos of *N. korthausae*, although the time course is very different.

Data presented in the present study and those of Levels et al. (1986) for *N. korthausae* indicate that diapause III is accompanied by depression of metabolic rate and can last for extended periods. In contrast, delayed hatching in embryos of *Fundulus heteroclitus* (DiMichele and Taylor, 1980; DiMichele and Powers, 1984) and the California grunion *Leuresthes tenuis* (Darken et al., 1998) is not associated with metabolic depression and is only a short-term delay. In fact, Darken et al. (1998) estimate that embryos of *L. tenuis* have sufficient energy to survive only one extra tidal cycle (9–13 days). Darken et al. (1998) suggest that, by maintaining a high metabolic rate, embryos of *L. tenuis* are always ready to hatch. The ability to hatch quickly may be beneficial in both *L. tenuis* and *F. heteroclitus* because the window for successful hatching is limited to each spring tide. In contrast, the long duration of the dry season and relative instability and unpredictability of ephemeral pond habitats may have favored diapause over delayed hatching in annual killifish.

CR ratios and metabolic biochemistry

CR ratios are often used to make inferences about the contribution of anaerobic processes to the total energy flow in an organism (e.g. Gnaiger, 1983; Gnaiger and Kemp, 1990). CR ratios between -443 and -478 kJ mol^{-1} O$_2$ are thought to represent completely aerobic metabolism (Gnaiger, 1983). This range in CR ratios is based on theoretical calculations of oxycaloric equivalents, which predict the amount of heat production expected per mole of oxygen consumed when a given metabolic substrate is completely oxidized to CO$_2$ and water. Many authors choose to use an oxycaloric equivalent value of -450 kJ mol^{-1} O$_2$ to represent aerobic metabolism of mixed substrates (Widdows, 1987). CR ratios markedly higher than the oxycaloric equivalent are thought to indicate the contribution of anaerobic pathways to total energy flow.

For developmental stages after diapause II in *A. limnaeus*, CR ratios indicate a largely aerobic metabolism (Fig. 8). These aerobic CR ratios agree with values reported for both early (Paynter et al., 1991) and late (Gnaiger, 1983; Finn et al., 1995) embryos of other teleost fish under aerobic conditions (for a review, see Hand, 1999). In contrast, embryos of *A. limnaeus* during early development and diapause II exhibit CR ratios well above the oxycaloric equivalent (Fig. 6). In cases of hypoxia, excess heat dissipation can be explained by the accumulation of end products such as lactate or ethanol (Gnaiger et al., 1981; van Waversveld et al., 1989; Johansson et al., 1995). However, in our studies, *A. limnaeus* embryos were not hypoxic. Nevertheless, there are a number of

examples where anaerobic processes contribute to the total energy flow of cells under normoxic conditions (for a brief review, see Gnaiger and Kemp, 1990). Lactate levels remained low and actually declined after 12 days post-fertilization (Fig. 13B), and ethanol was detected neither in acid extracts of embryos nor in the media in which embryos were incubated (data not shown). Because of the insignificant change in glycogen content, high CR ratios in *A. limnaeus* during early development and diapause II cannot be explained by the production of glycogen-derived end products. Although total protein content decreases by 22 % from 0 to 70 days post-fertilization, hydrolysis of protein to free amino acids can account for only approximately 2 % of the excess heat (based on -7 ± 2 kJ mol^{-1} peptide cleaved; Morowitz, 1968). A more thorough evaluation of possible metabolic end products and metabolic intermediates may clarify the reason for the high CR ratios observed in diapause II embryos.

Developing and diapause embryos of *A. limnaeus* maintain a highly charged adenylate pool as shown by high [ATP]/[ADP] ratios and high values for adenylate energy charge (Fig. 12). [ATP]/[ADP] ratios and adenylate energy charge for embryos of *A. limnaeus* are substantially higher than for other fish embryos. Boulekbache (1981) reports adenylate energy charge values of 0.72 in fertilized trout embryos, which then fall to values of 0.6 during early development. The adenylate energy charge for loach embryos during early development is 0.72, as calculated from the data of Milman and Yurowitzki (1967). [ATP]/[ADP] ratios are 1–2 in trout embryos (Boulekbache, 1981) and approximately 5 in loach (Milman and Yurowitzki, 1967). The maintenance of a high energy charge in diapause embryos of *A. limnaeus* is consistent with other organisms that enter diapause and suggests a tightly coupled down-regulation of energy-producing and energy-consuming processes. Embryos of *Artemia franciscana*, an organism that does not maintain high adenylate energy charge or [ATP]/[ADP] ratios during anaerobic quiescence, contain high levels of ATP during diapause, as shown by ^{31}P-NMR (Drinkwater and Crowe, 1987; Drinkwater and Clegg, 1991). As a likely consequence, these diapausing embryos do not experience the pronounced decrease in intracellular pH that is integrally associated with metabolic depression during anaerobic quiescence (for a review, see Hand, 1997). Thus, as a result of the high levels of adenylates in embryos of *A. limnaeus*, we predict that no major changes in intracellular pH occur during diapause II.

The substantial increase in [AMP]/[ATP] ratios after 8 days post-fertilization may have interesting implications for the regulation of metabolism in embryos of *A. limnaeus*. In recent reviews by Hardie and Carling (1997) and Hardie et al. (1998), the AMP-activated protein kinase (AMPK) has been implicated as a 'fuel gauge' and a 'metabolic sensor' in eukaryotic cells. The AMPK is thought to be regulated mainly by the [AMP]/[ATP] ratio; high ratios activate the kinase while low ratios cause inactivation. ATP and AMP probably compete for the same binding site (Ferrer et al., 1987), and raising [ATP] to 4 mmol l^{-1} results in a 10-fold increase in the AMP concentration required to activate AMPK (Corton et al., 1995). Activated AMPK is known to phosphorylate and deactivate three key biosynthetic enzymes: acetyl-CoA carboxylase (fatty acid synthesis; e.g. Vavvas et al., 1997), 3-hydroxy-3-methylglutaryl-CoA reductase (sterol synthesis; e.g. Sato et al., 1993) and glycogen synthase (Carling and Hardie, 1989). Interestingly, AMPK also phosphorylates Raf-1, which prevents activation of Raf-1 by protein kinase A (Morrison et al., 1993). Because Raf-1 is an important intermediate step in the activation of MAP kinases (Morrison and Cutler, 1997), this has led to speculation (Hardie et al., 1998) that AMPK may play a role in controlling cell proliferation.

The strong correlation between [AMP]/[ATP] ratios and a decrease in both indices of energy flow (Fig. 12B) suggests a role for this variable in the control of biosynthetic pathways and the associated ATP turnover in embryos of *A. limnaeus*. We estimate [AMP] in embryonic cells of *A. limnaeus* to be well over the activation threshold (>100 µmol l^{-1}) for the AMPK by 14 days post-fertilization despite high levels of ATP in these cells (approximately 1 mmol l^{-1}). In addition, [AMP]/[ATP] ratios in diapause II embryos are nearly an order of magnitude higher than values reported to activate AMPK in rat skeletal muscle (Hutber et al., 1997). The elevation of [AMP] in embryos of *A. limnaeus* probably arises from the small but significant decreases in [ATP] between 8 and 70 days post-fertilization. Adenosine is also known to be a potent signaling molecule and deserves evaluation in future studies of diapause in these embryos.

In summary, this paper describes some of the major physiological and biochemical characteristics of embryonic diapause in *A. limnaeus*. Embryonic diapause (diapause II and III) is accompanied by a substantial depression of metabolic rate that largely precedes the onset of developmental arrest at diapause II. An additional decline in the rate of oxygen consumption, but not in the rate of heat dissipation, during diapause II leads to CR ratios above the oxycaloric equivalent. Although [ATP]/[ADP] ratios are stable during early development, elevated levels of AMP may be important in regulating the depression of anabolic pathways and cell proliferation during diapause.

References

Bergmeyer, H.-U. (1974). *Methods of Enzymatic Analysis*. 3rd edition. New York: Academic Press.

Boulekbache, H. (1981). Energy metabolism in fish development. *Am. Zool.* **21**, 377–389.

Burton, K. (1956). A study of the conditions and mechanism of the diphenylamine reaction for the colorimetric estimation of deoxyribonucleic acid. *Biochem. J.* **62**, 315–323.

Carling, D. and Hardie, D. G. (1989). The substrate and sequence specificity of the AMP-activated protein kinase. Phosphorylation of

glycogen synthase and phosphorylase kinase. *Biochim. Biophys. Acta* **1012**, 81–86.

Carpenter, J. F. and Hand, S. C. (1986). Arrestment of carbohydrate metabolism during anaerobic dormancy and aerobic acidosis in *Artemia* embryos: determination of pH-sensitive control points. *J. Comp. Physiol.* B **156**, 451–459.

Clegg, J. S., Drinkwater, L. E. and Sorgeloos, P. (1996). The metabolic status of diapause embryos of *Artemia franciscana* (SFB). *Physiol. Zool.* **69**, 49–66.

Corton, J. M., Gillespie, J. G., Hawley, S. A. and Hardie, D. G. (1995). 5-Aminoimidazole-4-carboxamide ribonucleoside. A specific method for activating AMP-activated protein kinase in intact cells? *Eur. J. Biochem.* **229**, 558–565.

Darken, R. S., Martin, K. L. M. and Fisher, M. C. (1998). Metabolism during delayed hatching in terrestrial eggs of a marine fish, the Grunion *Leuresthes tenuis*. *Physiol. Zool.* **71**, 400–406.

DiMichele, L. and Powers, D. A. (1984). The relationship between oxygen consumption rate and hatching in *Fundulus heteroclitus*. *Physiol. Zool.* **57**, 46–51.

DiMichele, L. and Taylor, M. H. (1980). The environmental control of hatching in *Fundulus heteroclitus*. *J. Exp. Zool.* **214**, 181–187.

Drinkwater, L. E. and Clegg, J. S. (1991). Experimental biology of cyst diapause. In Artemia *Biology* (ed. R. A. Browne, P. Sorgeloos and C. N. A. Trotman), pp. 93–117. Boca Raton, FL: CRC Press.

Drinkwater, L. E. and Crowe, J. H. (1987). Regulation of embryonic diapause in *Artemia*: environmental and physiological signals. *J. Exp. Zool.* **241**, 297–307.

Ferrer, A., Caelles, C., Massot, N. and Hegardt, F. G. (1987). Affinity labeling of the catalytic and AMP allosteric sites of 3-hydroxy-3-methylglutaryl-coenzyme A reductase kinase by 5′-*p*-fluorosulfonylbenzoyladenosine. *J. Biol. Chem.* **262**, 13507–13512.

Finn, R. N., Widdows, J. and Fyhn, H. J. (1995). Calorespirometry of developing embryos and yolk-sac larvae of turbot (*Scophthalmus maximus*). *Mar. Biol.* **122**, 157–163.

Giles, K. W. and Myers, A. (1965). An improved diphenylamine method for the estimation of deoxyribonucleic acid. *Nature* **206**, 93.

Gnaiger, E. (1983). Heat dissipation and energetic efficiency in animal anoxibiosis: Economy contra power. *J. Exp. Zool.* **228**, 471–490.

Gnaiger, E. and Kemp, R. B. (1990). Anaerobic metabolism in aerobic mammalian cells: information from the ratio of calorimetric heat flux and respirometric oxygen flux. *Biochim. Biophys. Acta* **1016**, 328–332.

Gnaiger, E., Lackner, R., Ortner, M., Putzer, V. and Kaufmann, R. (1981). Physiological and biochemical parameters in anoxic and aerobic energy metabolism of embryonic salmonids, *Salvelinus alpinus*. *Eur. J. Physiol.* (Suppl.) **131**, R57.

Hand, S. C. (1991). Metabolic dormancy in aquatic invertebrates. *Adv. Comp. Env. Physiol.* **8**, 1–50.

Hand, S. C. (1997). Oxygen, pH$_i$ and arrest of biosynthesis in brine shrimp embryos. *Acta Physiol. Scand.* **161**, 543–551.

Hand, S. C. (1999). Calorimetric approaches to animal physiology and bioenergetics. In *Handbook of Thermal Analysis and Calorimetry*, vol. 4 (ed. R. B. Kemp). Amsterdam: Elsevier Science (in press).

Hardie, D. G. and Carling, D. (1997). The AMP-activated kinase. Fuel gauge of the mammalian cell? *Eur. J. Biochem.* **246**, 259–271.

Hardie, D. G., Carling, D. and Carlson, M. (1998). The AMP-activated/SNF1 protein kinase subfamily: metabolic sensors of the eukaryotic cell? *Annu. Rev. Biochem.* **67**, 821–855.

Hishida, T.-O. and Nakano, E. (1954). Respiratory metabolism during fish development. *Embryologia* **2**, 67–79.

Hutber, C. A., Hardie, D. G. and Winder, W. W. (1997). Electrical stimulation inactivates muscle acetyl-CoA carboxylase and increases AMP-activated protein kinase. *Am. J. Physiol.* **272**, E262–E266.

Jermyn, M. A. (1975). Increasing the sensitivity of the anthrone method for carbohydrates. *Analyt. Biochem.* **68**, 332–335.

Johansson, D., Nilsson, G. E. and Törnblom, E. (1995). Effects of anoxia on energy metabolism in crucian carp brain slices studied with microcalorimetry. *J. Exp. Biol.* **198**, 853–859.

Kwast, K. E. and Hand, S. C. (1996). Oxygen and pH regulation of protein synthesis in mitochondria from *Artemia franciscana* embryos. *Biochem. J.* **313**, 207–213.

Kwast, K. E., Shapiro, J. I., Rees, B. B. and Hand, S. C. (1995). Oxidative phosphorylation and realkalinization of intracellular pH during recovery from anoxia in *Artemia franciscana* embryos. *Biochim. Biophys. Acta.* **1232**, 5–12.

Levels, P. J. and Denucé, J. M. (1988). Intrinsic variability in the frequency of embryonic diapauses of the annual fish *Nothobranchius korthausae*, regulated by light:dark cycle and temperature. *Env. Biol. Fishes* **22**, 211–223.

Levels, P. J., Gubbels, R. E. M. B. and Denuce, J. M. (1986). Oxygen consumption during embryonic development of the annual fish *Nothobranchius korthausae* with special reference to diapause. *Comp. Biochem. Physiol.* **84**A, 767–770.

Lilyestrom, C. and Taphorn, D. (1982). El control biologico de mosquitos mediante peces en la cuenca del Lago de Maracaibo, Venezuela. *Informe Tecnico del Vice – Rectorado de Produccion Agricola* **6**, 1–38.

Loomis, S. H., Hand, S. C. and Fell, P. E. (1996a). Metabolism of gemmules from the freshwater sponge *Eunapius fragilis* during diapause and post-diapause states. *Biol. Bull.* **191**, 385–392.

Loomis, S. H., Ungemach, L. F., Branchini, B. R., Hand, S. C. and Fell, P. E. (1996b). Carbohydrate mobilization during germination of post-diapausing gemmules of the freshwater sponge *Eunapius fragilis*. *Biol. Bull.* **191**, 393–401.

Lowry, O. H. and Passoneau, J. V. (1972). *A Flexible System of Enzymatic Analysis*. London: Academic Press.

Mandoli, D. F., Ford, G. A., Waldron, L. J., Nemson, J. A. and Briggs, W. R. (1990). Some spectral properties of several soil types: implications for photomorphogenesis. *Plant Cell Env.* **13**, 287–294.

Markofsky, J. and Matias, J. R. (1977). The effects of temperature and season of collection on the onset and duration of diapause in embryos of the annual fish *Nothobranchius guentheri*. *J. Exp. Zool.* **202**, 49–56.

Markofsky, J., Matias, J. R., Inglima, K., Vogelman, J. H. and Orentreich, N. (1979). The variable effects of ambient and artificial light:dark cycles on embryonic diapause in a laboratory population of the annual fish *Nothobranchius guentheri*. *J. Exp. Biol.* **83**, 203–215.

Milman, L. S. and Yurowitzki, Yu. G. (1967). The control of glycolysis in early embryogenesis. *Biochim. Biophys. Acta* **148**, 362–371.

Milman, L. S. and Yurowitzki, Yu. G. (1973). Regulation of glycolysis in the early development of fish embryos. In *Monographs in Developmental Biology*, vol. 6 (ed. A. Wolsky). New York: S. Karger. 106pp.

Morowitz, H. J. (1968). *Energy Flow in Biology. Biological*

Organization as a Problem in Thermal Physics. New York: Academic Press. 96pp.

Morrison, D. K. and Cutler, R. E. (1997). The complexity of Raf-1 regulation. *Curr. Opin. Cell Biol.* **9**, 174–179.

Morrison, D. K., Heidecker, G., Rapp, U. R. and Copeland, T. D. (1993). Identification of the major phosphorylation sites of the Raf-1 kinase. *J. Biol. Chem.* **268**, 17309–17316.

Myers, G. S. (1952). Annual fishes. *Aquarium J.* **23**, 125–141.

Nico, L. G. and Thomerson, J. E. (1989). Ecology, food habits and spatial interactions of Orinoco Basin annual killifish. *Acta Biol. Venez.* **12**, 106–120.

Paynter, K. T., DiMichele, L., Hand, S. C. and Powers, D. A. (1991). Metabolic implications of *Ldh-B* genotype during early development in *Fundulus heteroclitus*. *J. Exp. Zool.* **257**, 24–33.

Peters, N. (1963). Embryonale Anpassungen oviparer Zahnkarpfen aus periodisch austrocknenden Gewässern. *Int. Rev. Ges. Hydrobiol.* **48**, 257–313.

Peterson, G. L. (1977). A simplification of the protein assay method of Lowry et al., which is generally more applicable. *Analyt. Biochem.* **83**, 346–356.

Podrabsky, J. E. (1999). Husbandry of the annual killifish *Austrofundulus limnaeus* with special emphasis on collection and rearing of embryos. *Env. Biol. Fishes* **54**, 421–431.

Podrabsky, J. E., Hrbek, T. and Hand, S. C. (1998). Physical and chemical characteristics of ephemeral pond habitats in the Maracaibo basin and Llanos region of Venezuela. *Hydrobiologia* **362**, 67–78.

Rees, B. B. and Hand, S. C. (1991). Regulation of glycolysis in the land snail *Oreohelix* during estivation and artificial hypercapnia. *J. Comp. Physiol.* B **161**, 237–246.

Sato, R., Goldstein, J. L. and Brown, M. S. (1993). Replacement of serine-871 of hamster 3-hydroxy-3-methylglutaryl-CoA reductase prevents phosphorylation by AMP-activated kinase and blocks inhibition of sterol synthesis induced by ATP depletion. *Proc. Natl. Acad. Sci. USA* **90**, 9261–9265.

Simpson, B. R. C. (1979). The phenology of annual killifishes. *Symp. Zool. Soc. Lond.* **44**, 243–261.

Tester, M. and Morris, C. (1987). The penetration of light through soil. *Plant Cell Env.* **10**, 281–286.

van Waversveld, J., Addink, A. D. F. and van den Thillart, G. (1989). The anaerobic energy metabolism of goldfish determined by simultaneous direct and indirect calorimetry during anoxia and hypoxia. *J. Comp. Physiol.* B **159**, 263–268.

Vavvas, D., Apazidis, A., Saha, A. K., Gamble, J., Patel, A., Kemp, B. E., Witters, L. A. and Ruderman, N. B. (1997). Contraction-induced changes in acetyl-CoA carboxylase and 5′-AMP-activated kinase in skeletal muscle. *J. Biol. Chem.* **272**, 13255–13261.

Walsh, W. A., Swanson, C., Lee, C.-S., Banno, J. E. and Eda, H. (1989). Oxygen consumption by eggs and larvae of striped mullet, *Mugil cephalus*, in relation to development, salinity and temperature. *J. Fish Biol.* **35**, 347–358.

Widdows, J. (1987). Application of calorimetric methods in ecological studies. In *Thermal and Energetic Studies of Cellular Biological Systems* (ed. A. M. James), pp. 182–215. Bristol: IOP Publishing.

Wourms, J. P. (1972a). Developmental biology of annual fishes. I. Stages in the normal development of *Austrofundulus myersi* Dahl. *J. Exp. Zool.* **182**, 143–168.

Wourms, J. P. (1972b). The developmental biology of annual fishes. II. Naturally occurring dispersion and reaggregation of blastomeres during the development of annual fish eggs. *J. Exp. Zool.* **182**, 169–200.

Wourms, J. P. (1972c). The developmental biology of annual fishes. III. Pre-embryonic and embryonic diapause of variable duration in the eggs of annual fishes. *J. Exp. Zool.* **182**, 389–414.